A minigoniometer for x-ray diffraction studies down to 4K on 4-circle diffractometers equipped with 2D detectors

Pierre Fertey, Roger Argoud, Pierre Bordet, Jacques Reymann, Cyril Palin, Christophe Bouchard, Rémy Bruyère, Emmanuel Wenger, Claude Lecomte

A minigoniometer for x-ray diffraction studies down to 4K on 4-circle diffractometers equipped with 2D detectors

Fertey Pierre,[a,b]* Argoud Roger,[c] Bordet Pierre,[c] Reymann Jacques,[a] Palin Cyril,[a] Bouchard Christophe,[c] Bruyère Rémi,[c] Wenger Emmanuel[a] and Lecomte Claude[a]

[a]*Laboratoire de Cristallographie et Modélisation des Matériaux Minéraux et Biologiques, UMR-CNRS-7036, Université Henri Poincaré - Nancy I, B.P. 239, 54 506 Vandoeuvre-lès-Nancy Cedex France,* [b]*Synchrotron Soleil, L'Orme des Merisiers, Saint-Aubin - B.P. 48, 91192 Gif-sur-Yvette Cedex France, and* [c]*Institut NEEL, CNRS and Université Joseph Fourier, BP 166, F38042 Grenoble Cedex 9 France.*

E-mail: pierre.fertey@synchrotron-soleil.fr

(Received 0 XXXXXXX 0000; accepted 0 XXXXXXX 0000)

Abstract

A 'universal' low temperature device for laboratory x-ray diffractometers equipped with 2D detectors has been developed. Single crystal data collections can be performed down to 4K. Due to an original design, the completeness of the data set is not affected by the limited number of accessible orientations of the sample. Classical structure analysis can therefore be performed as well as high resolution (high angle) studies for electron densities analysis. Derived from an idea of Argoud et al.(Argoud & Muller, 1989), the sample is mounted on a holder magnetically coupled to the diffractometer phi-axis. The coupling is achieved by mounting a master magnet in place of the usual goniometer head. This magnet drives a slave magnet fixed on the crystal holder: a two axis minigoniometer. This low temperature arrangement is adaptable to any kappa geometry single crystal diffractometer equipped with a 2D detector and can be placed into various types of cryostat. This paper reports the home made mechanical design and the performances of this device.

1. Introduction

The understanding of the correlations between the structure and the physical properties of materials is essential to clarify the mechanisms at the origin of these properties. X-ray diffraction is a unique tool to analyze structural properties of matter. Furthermore, from accurate (single crystal) X-ray diffraction data measured up to large momentum transfers ($sin\theta/\lambda > 1\mathring{A}^{-1}$), a detailed description of atomic structure, thermal vibrations and electron-density distributions can be reached. Their variation as a function of external perturbations is of prime interest when structural changes and the redistribution of the electron density that occur after a phase transition can be determined. The advantages of low temperature single crystal x-ray diffraction have long been recognised(Goeta & Howard, 2004). Experiments performed on single crystals at different temperatures down to about 100K can be done almost routinely, using nitrogen gas blowers. However, for lower temperatures, experimental devices allowing such experiments to be performed are not so commonly encountered. Three types of cryostat suited for 4-circles diffractometer are used: (i) cryostats rigidly attached to the goniometer head (i.e. to the crystal) and constrained to follow all the rotations, (ii) cryostats rigidly attached to the diffractometer, remaining stationary and (iii) full eulerian cradle completely enclosed within a cryostat.

Those of the first kind are generally met at synchrotron end stations where the diffractometers have robust rotation arms to support the load and large volume accessible around the sample. However, this solution implies a particular cryostat geometry to follow the diffractometer movements and mechanical constraints on the circles induced by the helium transfer lines. Furthermore, if thermal screens made of beryllium or carbon are used, the corrections of the crystal positions become tedious and the X-ray background level becomes relatively high and structured if the beam stop is not installed inside the sample chamber. Recently, Messerschmidt et al. overcame this drawbacks by developing a Kapton film vacuum chamber mounted on the cold head of a closed-cycle helium cryostat(Meserschmidt *et al.*, 2003).

The second type of cryostat is better adapted to laboratory diffractometers which are more compact and not robust enough to carry heavy loads. Open flow cryostats are typical examples:

the sample is cooled inside an open stream of dry helium gas. Room temperature-like strategies for data collection can be performed since almost no limitations of the orientations of the sample in the x-ray beam exist. However, the main drawbacks are the availability and cost of the helium (which cannot be recycled), a poor agreement between the temperature of the sample and that of the thermal sensor (due to the temperature gradient and the reduced volume where the temperature is homogenous), icing conditions, and the limited lowest temperature attainable (from 28K to 15K depending of the manufacturer)[1].

Very few cryostats are of the third kind: the sample orientation device is mounted completely inside the sample room of a helium cryostat. One example has been developed for single crystal neutron diffraction(Elf *et al.*, 1984). One of the authors has developed a magnetically coupled crystal holder (i.e. a mini 3 axes goniometer) for a four-circle x-ray diffractometer equipped with a point detector. The coupling is achieved by mounting a master magnet in place of the usual goniometer head. This magnet drives a slave magnet fixed on the minigoniometer enclosed into the sample chamber of a helium-flow cryostat(Argoud & Muller, 1989). This original solution combines the advantages of type (i) and type (ii) cryostat with only few restrictions on the orientations of the sample. However, this minigoniometer was made of quartz in order to reduce thermal contraction, which made it rather fragile and delicate to use. Furthermore, its design leads to large shadowed areas when used with a two dimensional detector.

When a two dimensional detector is used, the number of orientational degrees of freedom of the sample can be reduced. The diffraction process is indeed not limited to the equatorial plane (i.e. the horizontal plane for a laboratory diffractometer): two rotation axes are in principle enough to measure a complete data set. Therefore, following the idea of Argoud and Muller, we have developed a device adapted to x-ray diffractometers with kappa geometry and equipped with a 2D detector. Our system is an evolution of their original design: a 2 rotation axes minigoniometer has been permanently installed into the sample chamber of a helium bath cryostat. Our apparatus can be adapted to any kind of such kappa diffractometer. The minigoniometer

[1] See for example:http://www.cryoindustries.com/CRYSTAL.htm, http://www.oxfordcryosystems.co.uk/helix/home.html, http://www.oxford-diffraction.com/cryo.asp

can be placed inside various types of cryostats (helium-bath, continuous flow, closed-cycle). It can also be used in many other applications like controlled-atmosphere, moderate pressure or vacuum investigations.

In this paper the apparatus consisting of the minigoniometer, an optical cryostat and the cryostat holder are successively described. The performances are then illustrated.

2. The Setup

A simplified schematic view of the device is reported on Figure 1. The orientation of the sample in the x-ray beam is driven by a magnetic coupling through the walls of the cryostat between a slave magnet attached to the minigoniometer inside the cryostat and a master magnet mounted on the phi axis on the kappa arm of the diffractometer in place of the usual goniometer head. We have installed this system on a Nonius 4-circle KCCD diffractometer as shown on Figure 2. Figure 3 displays a picture of the sample nacelle carrying the minigoniometer. The main characteristics of the device are reported in Table 1.

2.1. The magnetically coupled minigoniometer

2.1.1. The sample holder The sample can be oriented in the incident x-ray beam by the two omega and phi rotation axes of the minigoniometer. The slave magnet is attached to the phi axis. These two axes intersect at a point which must coincide with the center of the host diffractometer. The sample is glued onto an exchangeable silica rod which coincides with the phi axis, at the center of rotation of the minigoniometer and therefore of the host diffractometer.

The angle between the phi and omega axes has been fixed at 45 $^{\circ}$. In this configuration, the master magnet can not enter in collision with the incident beam collimator. Data collection strategies are elaborated at fixed chi ($\pm$45 $^{\circ}$) from omega scans at different values of phi or phi scans at different values of omega. The values of the phi angle are not limited contrary to the omega angle. However, a 101 $^{\circ}$ to 123 $^{\circ}$ omega rotation is accessible depending on the phi value.

We used micromechanics techniques[2] to meet the rather stringent mechanical requirements: (i)system confined inside a small volume ($\approx$ sphere of 50 mm diameter), (ii) common intersection of the two rotation axes within $\pm 0.01\ mm$, (iii) all parts non magnetic (except the slave magnet), (iv) thermal contraction effects between the room-temperature and 4.2 K as small as possible (in particular, the tolerance in the intersection of the two axes must not be degraded), and (v) very low frictions to allow a reliable magnetic coupling. For examples, the core of the minigoniometer is made of tantalum alloy. The rotation axes are made of tungsten carbide and rotate on stainless steel ball bearings.

In order to prevent the contamination of the images from spurious diffraction/diffusion effects, a beam stop and an antiscattering tube have also been incorporated in the sample nacelle as illustrated on Figure 2. They are mounted on the same holder which can be rotated around an axis superimposed on the omega axis of the minigoniometer. Therefore, the position of the beam stop/antiscatterer is easily and manually aligned from outside of the cryostat.

A led is also attached to the beam stop holder to light the sample for a visual adjustment of its centering on the diffractometer as will be explained below.

2.1.2. The magnets The magnetic field of the master magnet and its gradient, near the slave magnet, must be as high as possible so that the sample holder can follow the ϕ rotations (high magnetic coupling) and the ω rotations (high attractive force) and overcome the frictions as small as they may be.

The design of the master magnet was inspired form Argoud et al.(Argoud & Muller, 1989). However, in order to decrease the magnet size and improve the remanent magnetization, the core of this new magnet is made of neodymium iron boron. The ends of the master magnet are machined in soft iron (cf. Figure 1). The slave magnet is made of AK502 magnetic alloy and is highly magnetized in the master magnet magnetic field.

Due to the strong magnetic field of the master magnet ($\approx$ 70 mT at the position of the

[2] Poinsard Design and Tools SA, ZAC de Besanon-Valentin, 25480 Misery-Salines, France

center of the slave magnet), the earth's magnetic field (0.05 mT) which is superimposed on the master magnet field can be neglected.

2.2. Cryostat

In our case, the sample nacelle is attached at the end of the sample stick which is introduced into a top load helium cryostat. We have chosen a helium bath orange cryostat from AS Scientific Products Ltd[3]. The cryostat was modified such that the effects of length contractions on the sample position during the cooling are minimized : the mechanical reference is now taken at the closest position of the cold finger, preventing an upward translation of the sample chamber on cooling (in the standard Orange cryostat, the mechanical reference is near the top of the cryostat).. A low pressure of helium gas in the sample nacelle ensures the cooling and a homogeneous temperature of the sample.

As can be seen on Figure 1 and 2, special tails have been designed. Three concentric tails are successively encased: the so-called room-temperature (stainless steel), intermediate (copper thermal screen) and helium (Cu OFHC) tails. A flat part was arranged in each tail to minimized the sample-to-detector distance: the shortest sample-to-detector distance is therefore 35 mm, offering a wide angle coverage of the reciprocal space (e.g. the largest angular opening of the cone of diffraction is about 86 $^{\circ}$ at 35 mm). An hemispherical dome ends each tail in order to keep a constant distance between the master and slave magnets during the movements of the goniometer. Furthermore, small entrance windows and a large exit window were also arranged. Seven holes (diameter 6 mm) for the incoming X-ray beam were bored every thirty degrees on the opposite part of the exit windows. On the room-temperature and helium tails, the holes were covered with a 100 μm transparent mylar film. The exit windows are broad rectangular apertures on the flat part of the cryostat tails($\approx 30 \times 30\ mm^2$). The room-temperature, intermediate and helium tail exit windows are respectively made of 300 μm beryllium, 10 μm aluminized mylar film and 100 μm aluminized kapton film.

During operation, the cryostat exit windows will always be made parallel to the detector

[3] www.assientific.co.uk

entrance window. Therefore, all procedures used to correct the effect of the detector entrance window on the diffraction images can also take into account the effect of the cryostat exit windows.

When introduced into the cryostat, the sample nacelle is brought in contact with the bottom of the helium tail ensuring the correct positioning of the sample inside the cryostat.

2.3. Cryostat holder

A mechanical support has been developed which allows accurate positionings of the cryostat onto the host diffractometer: (i) XYZ motorized translation motions (accuracy $\pm 2\ \mu m$) to superimposed the centers of the minigoniometer and of the diffractometer, (ii) two manual tilt rotations ($\pm 3\ ^{\circ}$) so that the omega axes of the minigoniometer and of the diffractometer can be set parallel, and (iii) a $30\ ^{\circ}$ step rotation around the omega axis for high angle data measurements. An extra rotation of the cryostat holder around the Z axis and a long range vertical translation of the cryostat have been added to completely retract the device when it is not used.

3. Operation

3.1. Mounting the sample

The sample is glued on a silica rod using bee wax, which is known not to exert stresses on the crystal when the temperature is lowered (Argoud & Muller, 1989). The silica rod is then introduced in the hollow phi axis previously filled with silicon grease and manually adjusted with a specific device under a microscope, so that the sample is exactly placed at the center of the minigoniometer. Furthermore, the crystal remains at the center during the hardening of the silicon grease.

3.2. Alignment

The cryostat centering procedure consists in two adjustments: (i) make the omega axes of the minigoniometer and of the diffractometer parallel (ii) superimpose the center of the

minigoniometer and the center of the diffractometer. Both axes are independently set in the vertical direction (adjustment screws of the base of the diffractometer basement, tilt rotations of the cryostat). In a first approximation, the omega axis of the minigoniometer and the revolution axis of the cryostat are supposed to be parallel by construction. To accurately locate the center of the diffractometer, a perfect stainless steel spherical ball is first mounted and precisely centered on the diffractometer in the usual way. Its position is then located with a second microscope attached to the arm of the detector. This position will be the reference position on which the crystal placed inside the cryostat must be superimposed. The cryostat (i.e. the sample) is then roughly centered on the diffractometer. Due to the transparent entrance windows of the tails, the crystal mounted on the minigoniometer inside the cryostat can be visualized with the second microscope. Therefore, the centering of the crystal on the diffractometer can be performed in the usual way using the XYZ translations of the cryostat holder. Figure 4 schematically describes the centering procedure in the X and Y directions. Thanks to the rotatable diode within the cryostat, the lighting of the sample can be enhanced for each position of the microscope.

3.3. Performances

3.3.1. Performances of the cryostat At the first cooling of the cryostat, the liquid helium temperature can be reached within 2h. The temperature sensor is located in the cold finger of the cryostat. The absolute temperature at the sample site was checked from the structural phase transition of $DyVO_4$. This compound undergoes a tetragonal-to-orthorhombic phase transition at $T_c = 14\ K$ (Cooke *et al.*, 1970; Cooke *et al.*, 1971). Since twining occurs because of the change of crystal system on cooling below the transition temperature, the $hh0$ Bragg reflections appear as split in the orthorhombic phase and the transition can easily be evidenced. The effective transition temperature was deduced from the measure of the full width at half maximum of the 660 Bragg reflection as function of temperature, as illustrated on Figure 5: the temperature difference between the sensor and the crystal temperatures was estimated to be

less than 0.5K. Furthermore, the thermal fluctuations at the regulator sensor does not exceed $\pm 0.03K$.

With an optimal adjustment of the cryostat, a 55 hours autonomy could be reached at 12 K and a 35 hours autonomy at 4K, between two successive refillings of the liquid Helium reservoir. However, for longer experiments, the Helium reservoir can be refilled without significant change of the sample temperature ($\pm 1K$).

3.3.2. Accuracy of the minigoniometer All the tests were made with a spherical yttrium iron garnet crystal ($\varnothing = 160\ \mu m$) which has long been used as a (local) reference sample when testing the performances of our low temperature devices. It has a cubic symmetry (i.e. many equivalent reflections for a given hkl) and does not display structural phase transition down to 4.2 K. The mechanical frictions of the minigoniometer have been evaluated by the measurement of the hysteresis introduced in the rocking curves of several Bragg reflections, measured as a function of the scan directions. The rocking curves were reconstructed from step rotations of the crystal passing through the diffracting conditions ($\Delta\omega$ or $\Delta\varphi = 0.1^{\circ}$). At each omega (phi) step, a 0.1° single pass rotation image was recorded and the raw diffracted intensity for the Bragg reflection of interest was evaluated. The procedure was repeated at low temperature and when the same crystal was mounted on a standard goniometer head and the cryostat removed from the host diffractometer. From the comparison between the rocking curves measured with and without the minigoniometer or as a function of the temperature, no extra shift could be evidenced as resulting from the frictions of the minigoniometer. Therefore, the driving of the sample via the magnetic coupling does not degrade the mechanical accuracy of the omega (phi) rotations of the host diffractometer.

3.3.3. Data collection A data collection was performed on the prototype organic charge transfer compound tetrathiafulvalene-p-chloranil (TTF-CA; $C_6S_4H_4 - C_6Cl_4O_2$), using graphite monochromatized MoK_α radiation on a Nonius KappaCCD diffractometer equiped with the

low temperature system described above. The TTF-CA complex is built from a mixed stacking of planar donor (D=TTF) and acceptor (A =CA) molecules. It undergoes a first-order neutral-to-ionic phase transition at $T_c = 82\ K$ (Torrance *et al.*, 1981; Garcia *et al.*, 2007): an increase of the charge transfer from the donor to the acceptor molecule is observed, associated with a dimerization of the organic stacks and the loss of inversion symmetry ($P2_1/n$ to Pn space group) (Garcia *et al.*, 2007; LeCointe *et al.*, 1995).

Due to its low symmetry, this compound was a good candidate to test the completeness of a data set. Experimental details are summarized in Table 2. 385 frames were collected at 12 K by performing four omega scans and one phi scan at the single kappa value fixed by the minigoniometer geometry (2 $^\circ$ / frame, exposure = 10 s/ $^\circ$). The detector was positioned at 15 $^\circ$ from the incident beam direction. A 0.8 $\mathring{A}^{-1}$ resolution was achieved with this configuration, which is sufficient for structure solution purposes. A 94% completeness was reached for this monoclinic compound. Integration of frames and data reduction were performed with DENZO (Otwinowski & Minor, 1997). The multiple integrated reflections were averaged using SORTAV (Blessing, 1987) adapted to area detector data. Internal agreement factors for all data are given in Table 2. The structure refinement was performed using the SHELX suite. Only reflections having $I > 2\sigma(I)$ were used in the structure least-squares refinements.

The results obtained could be compared to the structure refinement performed with a data set collected at 15 K on another crystal of the same compound using an Oxford diffraction Xcalibur diffractometer. In this case, the sample was cooled with an open stream helium gas. Details of this study have been published elsewhere (Garcia *et al.*, 2007). Within 3 sigma, the atomic coordinates of both studies are highly consistent (cf. supplementary material). Thermal parameters may differ slightly but this could be due to the different resolution of the two data sets (0.8 $\mathring{A}^{-1}$ in this study vs 1.16 $\mathring{A}^{-1}$ in the analysis of Pilar et al. (Garcia *et al.*, 2007)). Figure 6 shows the residual electron density in the CA plane. Despite the modest resolution of the data set and although the absorption corrections have not been performed, the residual density is mainly concentrated in between atoms giving a first indication of the deformation

density due to chemical bonds.

4. Conclusion

We have presented the characteristics and performances of an 'universal' device to be installed on a laboratory kappa geometry X-ray diffractometer equipped with a 2D detector. It allows to perform single crystal data collections down to 4K at low cost, with a temperature stability and accuracy usually not allowed by other systems. The sample is mounted on a two axes minigoniometer installed inside the sample chamber of a top load helium bath cryostat. Thanks to a magnetic coupling between a slave magnet attached to the phi axis of the minigoniometer and a master magnet mounted in place of the usual goniometer head on the host diffractometer, the orientation at low temperature of the sample in the x-ray beam can be achieved. A test data collection performed on a low symmetry crystal has demonstrated the relevance of this device: classical structure analysis as well as high resolution (high angle) data collection can be performed, which are particularly suited for electron densities analysis.

Two other examples illustrating the relevance of this setup for the accurate determination of the behavior of the cell parameters as a function of the temperature at a phase transition have alreday been published (Garcia *et al.*, 2005; Garcia *et al.*, 2007).

Acknowledgements

The authors thank P. Garcia and S. Dahaoui for providing the TTF-CA test crystal and CNRS for financial support.

Table 1. *Main characteristics of the apparatus.† Helium tail and thermal screen. ‡ room-temperature tail. *** pumped helium.*

ω rotation range	from 101 ° to 123 ° depending on ϕ
ϕ limit	none
$2\theta_{max}$	~ 133 °
Intersection of the two rotation axes	within 0.02 mm diameter sphere
Entrance X-ray windows	Mylar $\oslash = 6mm \times 100\mu m$
Exit X-ray windows	aperture ≈ 48 ° hor. $\times 49$ ° ver.
	Al-coated mylar† $20\mu m$
	Be‡ $300\mu m$
Centering of the crystal	visual, possible at all temperature
Accuracy of the crystal position	as a standard goniometer head
Lowest temperature	not tested but ≤ 4.2 K***
Temperature accuracy	0.5 K
Temperature stability	± 0.03 K
Liquid Helium consumption	0.12 $l.h^{-1}$ at 12 K
	0.19 $l.h^{-1}$ at 4.2 K
Diffractometer mechanical modifications	short collimator

Table 2. *Experimental details on the TTF-CA data collection and structural refinement.*

	TTF-CA
Temperature	12 K
Crystal system	monoclinic
Space group	Pn
Radiation type	sealed tube graphite monochromatized $MoK\alpha$
Reflections collected	17246
$I \geq 3\sigma$	62.5 %
Independent reflections	3251
Redundancy	4.7
$sin(\theta/\lambda)_{max}$	0.80 $\mathring{A}^{-1}$
mean I/σ	8.4
R_{int}	5.22 %
Completeness	94.3 %
$R(I > 2\sigma)$	3.66 %
max residual density	0.69 $e/\mathring{A}^3$

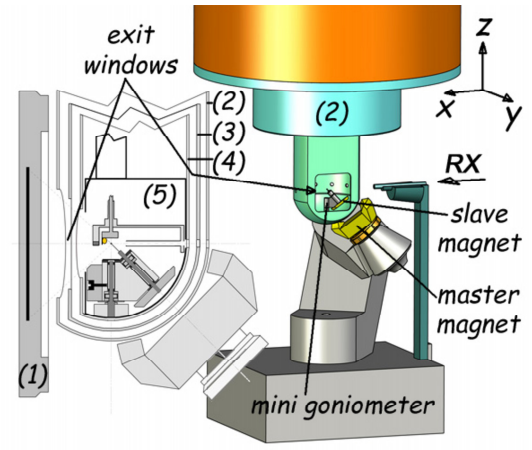

Fig. 1. Simplified schematic view of the magnetically coupled minigoniometer when the cryostat is rotated -90°. The master magnet is mounted in place of the usual goniometer head. Insert: drawing cut of the low part of the cryostat when the detecor (1) is at the closest distance from the sample. (2) room temperature tail and its Be window, (3) intermediate tail and its aluminized mylar window, (4) helium tail and its aluminized kapton window, (5) sample nacelle.

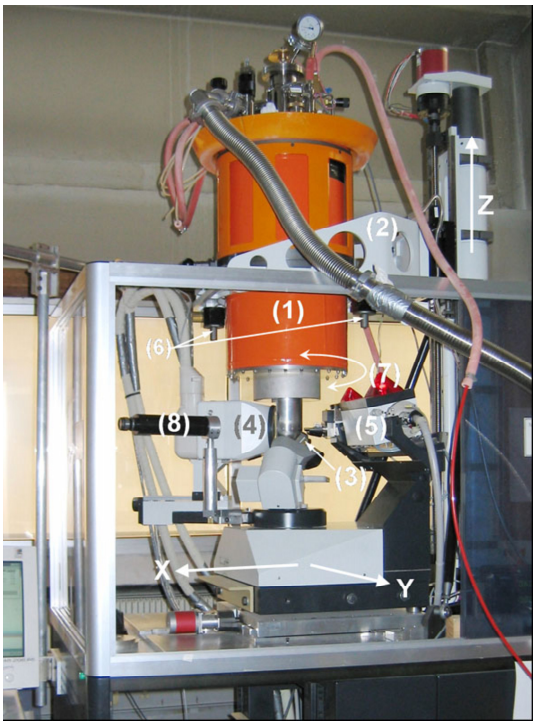

Fig. 2. Picture of the device installed on a Nonius K-CCD diffractometer. (1) orange cryostat, (2) cryostat holder, (3) master magnet, (4) CCD detector, (5) X-ray source, (6) tilt rotations, (7) main rotation, and (8) microscope.

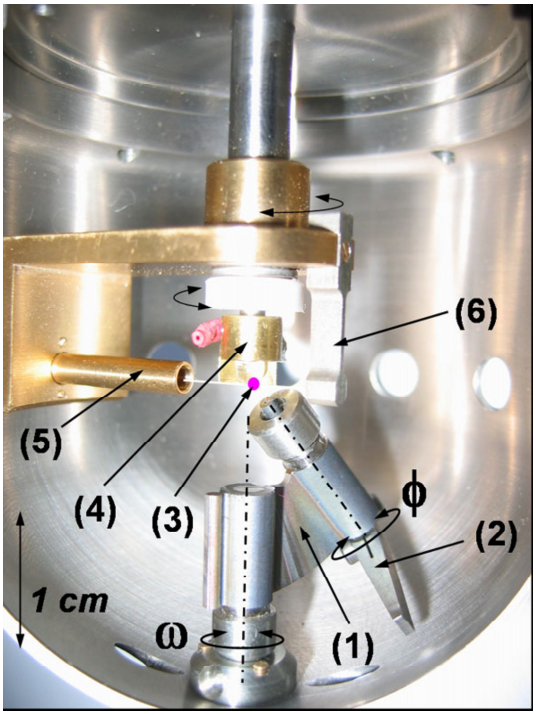

Fig. 3. Picture of the sample nacelle: (1) minigogiometer, (2) slave magnet, (3) sample, (4) diode, (5) antiscatterer, and (6) beam stop.

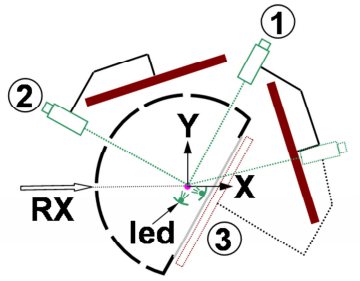

Fig. 4. Schematic representation of the centering procedure: (1) and (2) are two successive orthogonal orientations of the microscope. X and Y translations are performed to adjust the centering of the sample at the host diffractometer center. Position (3) is the detector position during the data collection.

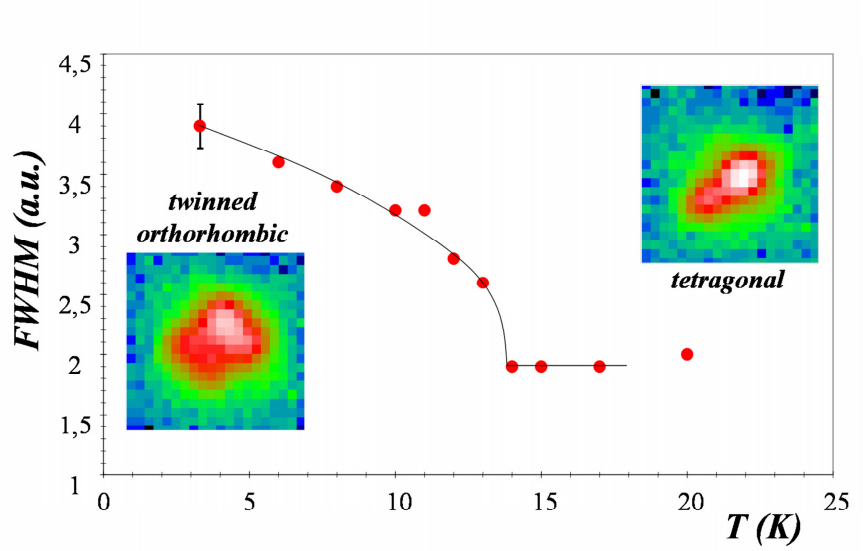

Fig. 5. Variation of the FWHM of the 660 reflection across the tetragonal-to-orthorhombic transition. The line is a guide for the eyes.

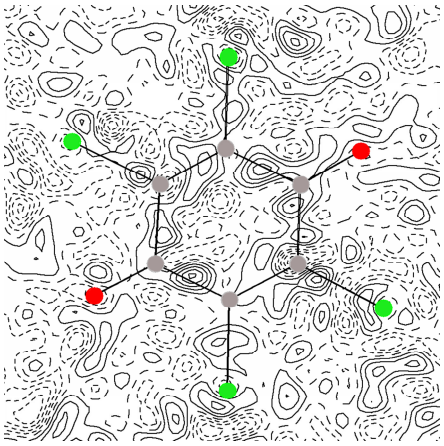

Fig. 6. Residual electron density in the $C_6Cl_4O_2$ molecule plane. Isocontours 0.1 $e.A^{-3}$.

References

Argoud, R. & Muller, J. (1989). *J. Appl. Cryst.* **22**, 584–591.

Blessing, R. H. (1987). *Crystallogr. Rev.* **1**, 3–326.

Cooke, A. H., Ellis, C. J., Gehring, K. A., Leask, M. J. M., Martin, D. M., Wanklyn, B. M., Wells, M. R. & White, R. L. (1970). *Solid State Commun.* **8**, 689–692.

Cooke, A. H., Martin, D. M. & Wells, M. R. (1971). *Solid State Commun.* **9**, 519–522.

Elf, F., Will, G., Chatzipetros, J. & Dujka, B. (1984). *Rev. Phys. Appl.* **48**, 793–794.

Garcia, P., Dahaoui, S., Fertey, P., Wenger, E. & Lecomte, C. (2005). *Phys. Rev. B*, **72**, 104115.

Garcia, P., Dahaoui, S., Katan, C., Souhassou, M. & Lecomte, C. (2007). *Faraday Discussions*, **135**, 217–231.

Goeta, A. & Howard, J. (2004). *Chem. Soc. Rev.* **33**, 490–500.

LeCointe, M., Lemee-Cailleau, M., Cailleau, H., Toudic, B., Toupet, L., Heger, G., Moussa, F., Scheiss, P., Kraft, K. H. & Karl, N. (1995). *Phys. Rev. B*, **51**, 3374–3386.

Meserschmidt, M., Meyer, M. & LugerBursill, P. (2003). *J. Appl. Cryst.* **36**, 1452–1454.

Otwinowski, Z. & Minor, M. (1997). *Methods in Enzymology, Macromolecular Crystallography, part A*, **276**, 307–326.

Torrance, J. B., Girlando, A., Mayerle, J. J., Crowley, J. I., Lee, V. Y., Batail, P. & Laplaca, S. J. (1981). *Phys. Rev. Lett.* **47**, 1747–1750.

Table 3. *Supplementary material: interatomic distances (in Å) of the TTF-CA molecule*

bond name	this study	Garcia et al. (2007)
	TTF	
C2-C9	1.388(5)	1.388(2)
C9-S11	1.740(6)	1.742(2)
C9-S12	1.755((4)	1.742(2)
C2-S5	1.740(6)	1.744(2)
C2-S4	1.748(4)	1.744(2)
C1-C3	1.346(6)	1.348(3)
C8-C10	1.331(6)	1.349(4)
	CA	
C15-O18	1.239(4)	1.238(3)
C21-O24	1.237(4)	1.238(3)
C23-Cl26	1.715(3)	1.717(2)
C22-Cl25	1.725(4)	1.721(2)
C17-Cl20	1.728(4)	1.718(2)
C16-Cl19	1.714(3)	1.723(2)
C17-C16	1.377(5)	1.367(3)
C16-C15	1.476(4)	1.480(3)
C15-C23	1.487(5)	1.483(3)
C23-C22	1.338(5)	1.366(3)
C22-C21	1.483(4)	1.482(3)
C21-C17	1.470(5)	1.481(3)

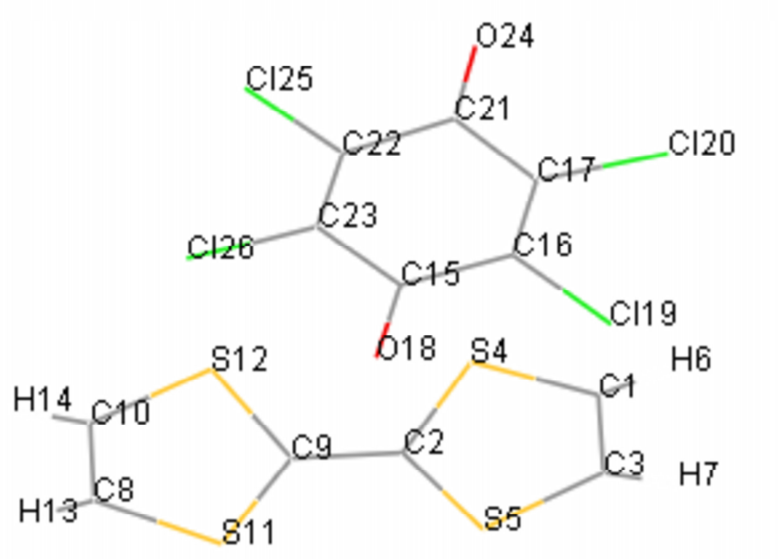

Fig. 7. Atom labels of the TTF-CA molecule.

Synopsis

A new helium based cryostat is described to be adapted on kappa diffractometers equiped with 2D detectors.